Design of Ground Penetrating Radar Antenna for Monitoring Soil Contamination at L Band Frequencies

T.Yathavi[1], B.Premalatha[2], K.M.Priya[3] and I.S.Akila[4]
[1]Faculty of Electronics and Communication, Coimbatore Institute of Technology, Coimbatore, Tamil Nadu, INDIA
[2]Faculty of Electronics and Communication, Coimbatore Institute of Technology, Coimbatore, Tamil Nadu, INDIA
[3]Faculty of Electronics and Communication, Coimbatore Institute of Technology, Coimbatore, Tamil Nadu, INDIA
[4]Faculty of Electronics and Communication, Coimbatore Institute of Technology, Coimbatore, Tamil Nadu, INDIA

[1]Corresponding Author: yathavi@cit.edu.in

Received: 18-11-2023 Revised: 01-12-2023 Accepted: 19-12-2023

ABSTRACT

A major concern for oil companies is the maintenance of oil pipelines. The contamination of the soil is caused by oil leaks from underground pipelines. Using GPR, contaminated soil sites can be located and characterized rapidly and relatively inexpensively without fracturing or spreading contamination. The antenna system is one of the most critical hardware components for GPR performance. To detect soil contamination, an L-band pyramidal horn antenna is designed and simulated at frequencies between 1 and 2 GHz. Modelling the electromagnetic fields in different soil types is done using a prototype GPR system setup. In order to carry out simulations during the design process, the dielectric permittivity of soil is measured and analytically represented by the Debye relaxation model. It is most important to detect contamination by comparing the dielectric permittivity of contaminated and uncontaminated soils. In terms of investigating soil contamination, GPR has proven very successful.

Keywords-- Soil Contamination Detection, L-Band Frequency, Ground Penetrating Radar, Permittivity Measurement, Pyramidal Horn Antenna Design

I. INTRODUCTION

The rusting and leakage of underground pipelines can cause soil contamination. The pipelines are at risk of leaks and spills. When pipelines are not maintained properly, leaks may occur into the surrounding environment, which could contaminate the soil. In underground piping systems, cracks, drilling, and corrosion are the most common causes of leaks [1]. It is sometimes difficult to locate contamination because it can spread over large areas. In order to detect oil leaks from underground pipelines, different techniques have been developed [2]. Drilling, soil sampling, and laboratory testing are required for leak detection using invasive techniques. It is possible for these methods to contribute to the spread of contaminants in polluted areas. Non-invasive techniques provide rapid characterization of contamination without creating cracks and are relatively simple and inexpensive.

Ground penetrating radar (GPR) is a non-destructive tool for non-invasive investigations [3]. GPR is a geophysical technique that maps the dielectric properties of the subsurface [4]–[5]. The method involves measuring the electromagnetic pulses that are transmitted into the medium and then collected by the receiver. The transmitter and receiver are both placed on the antenna [6]. A GPR system's ability to detect soil contamination depends on the contrast between clean and contaminated soils electrical properties [7]. Direct measurement of the dielectric properties of soil contamination is, therefore, effective in detecting contamination.

Radar antennas for ground-penetrating radar are commonly located near the surface of the soil or in contact with it. Consequently, the performance of GPR antenna systems, such as operating frequency, transmitted power, and antenna beamwidth, is directly dependent on soil properties. An optimal antenna design should be capable of performing consistently in a variety of soil types and weather conditions. Typically, GPR is used on dry soils since high radio frequencies are capable of reaching a particular depth [10]. Radar antennas are capable of detecting contaminants based on both their depth of penetration and frequency [11]. Operating frequencies of GPR systems are a trade-off. Despite low frequencies, soil contamination is not detectable at low frequencies because of their poor penetration and low resolution. The depth of penetration into moist soil is typically only a couple of centimeters, although contamination can be detected at higher frequencies.

Following is the organisation of the paper. The "Prototype model and dielectric modelling" section presents a prototype soil model for evaluating the effectiveness of GPR technology. The situation involves a plastic tube buried in soil and filled with lubricant oil. Two scenarios are considered: one where the soil beneath the pipe is dry sand, and the other where the soil beneath the pipe is contaminated with oil due to pipe leaks. In the section on "GPR antenna design", two identical wideband pyramidal horn antennas operating at L-band frequencies are designed to show that microwave sensing can discriminate between contaminated and clean soils precisely. "A summary of results" is presented in the "Conclusions" section.

II. PROTOTYPE MODEL AND DIELECTRIC MODELING

GPR technology can be used to detect soil contamination caused by leakage from oil pipelines, which is the primary objective of this work. It is necessary to design and simulate a prototype model in order to achieve this objective. In the prototype model, sand is loaded into a wooden box with a plastic pipe containing oil encased in soil. The model geometry is shown in Fig.1, and the optimised dimensions, found to provide the best performance, are listed in Table.1. For the prototype model shown in Fig.1, dielectric modelling of the mediums of interest is required. Microwaves propagate through soil based on its dielectric permittivity. It is possible to measure the dielectric permittivity of soil to detect pollutants effectively [12].

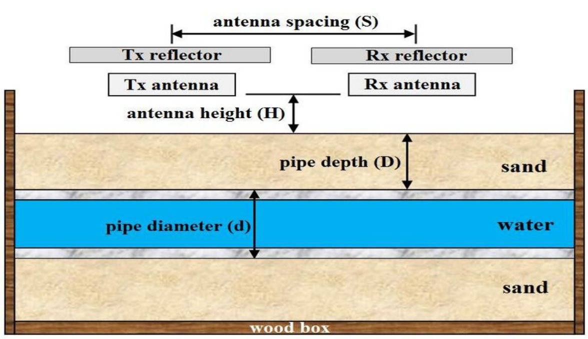

Figure 1: Soil contamination detection prototype model

Table 1: Optimized Dimensions of Model

Parameter	value (cm)
wooden box length	150
wooden box width	100
wooden box height	100
antenna height from ground surface (H)	10
antenna spacing (S)	50
pipe burial depth (D)	40
pipe diameter (d)	10
antenna tilting from vertical	22°

Making sure that specifications are maintained in an accurate and timely manner GPR is homodyne-based, which detects the oscillation by comparing it with a standard oscillation, which would be identical to the oscillation if it carried null information. In order to detect an oscillating signal, the phase and frequency modulations of the signal are extracted. Homodyne detection using frequency-modulated techniques uses a single frequency instead of two frequencies in heterodyne detection. Subsurface images are captured using radar pulses. As shown in Fig.1, Using electromagnetic radiation in the L band of the radio spectrum, this nondestructive method detects reflected signals from subsurface structures.

Materials' dielectric permittivity can be measured in the microwave range using different techniques. Among the techniques used are transmission line systems (free space, coaxial, and waveguide), cavity, and impedance techniques [13]. The complex dielectric permittivity of soil samples was measured with a Dielectric Assessment Kit (DAK). In the microwave frequency range, the DAK system provides simple, accurate, and convenient dielectric measurements. Fig.2 illustrates the experimental setup of the DAK measurement system. In the DAK setup, there is a Vector Network Analyzer (VNA), an open-ended coaxial probe, and a computer programme. The DAK probe has a 50-ohm impedance, and it should be calibrated using a long short circuit and a permittivity sample of known permittivity. To measure the complex reflection coefficient at the end of a coaxial line probe, the probe end is connected to a VNA.

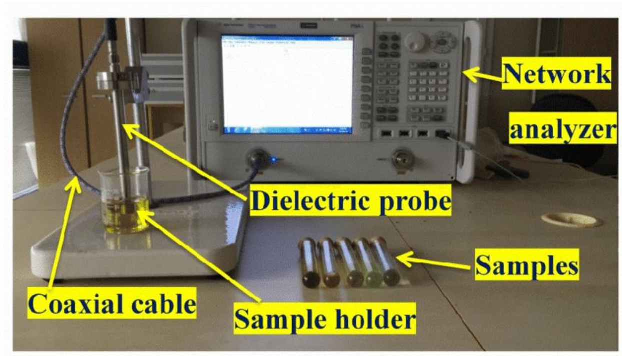

Figure 2: Experimental measurement system setup to measure soil samples

It is essential that the soil medium around the probe tip be smooth and homogeneous in order to prevent phase distortions caused by cable movements. Using DAK Software, the measured reflection coefficient is converted into the sample's complex permittivity. To avoid any reflections from the sample's boundary that might affect measurements, the sample volume should be large and homogeneous. DAK at room temperature is used to measure complex dielectric permittivity as a function of frequency in clean and contaminated sandy soil samples. As a result, soil samples are fitted with the Debye relaxation model [14] and [15].

$$\varepsilon = \varepsilon_\infty + \frac{\varepsilon_s - \varepsilon_\infty}{1 - if/f_0} + ia'' \quad —(1)$$

where εs is the static permittivity of soil, is an extrapolated permittivity at high frequencies, fo is the resonance frequency, i is the complex number symbol i =, and is an estimate of the sand losses presented as an imaginary part. A curve fitting routine is implemented using MATLAB software to find the most suitable Debye relaxation parameters. Based on the least squares method, the search algorithm is performed. Data fitting aims to find the Debye relaxation model values that are closest to the measured values. In Table.2, all measured soil samples are listed with their best Debye fitting parameters. For extrapolating permittivity to higher frequencies, researchers often use relaxation models. It could be possible to predict the dielectric properties of materials over a desired frequency range using a relaxation model, provided the model parameters are selected appropriately.

Table 2: Debye values of Two Different Sandy Soils

Soil Type	**Uncontaminated sandy soil**	**Contaminated sandy soil**
ε_s	2.51	5.68
ε_∞	2.82	5.99
fo (GHz)	0.249	0.412
a''	0.003	0.285

Microwave frequencies determine the dielectric permittivity of dry natural soil samples based on their physical components. Adding lubricant oil to sandy soil will result in oil infiltrating deeply into the soil and replacing air in pore spaces. The soil properties become more similar to those of the lubricant oil, so its chemical and physical properties will also be affected, affecting its dielectric permittivity. Fig.3 shows the experimentally measured values and the fitted data of the dielectric constant and the dielectric loss for both clean and oil-soil-contaminated samples. The measurements indicate an increase in both the dielectric constant and the dielectric loss factor due to the presence of lubricant oil. As a result, the Debye model parameters will reflect this contrast in dielectric properties.

It is clear that the dielectric properties of contaminated soil samples have changed significantly. By sensing the contrast between the reflected signals of clean and contaminated soils, ground penetrating radar (GPR) can detect contamination. There must be sufficient signal penetration for GPR equipment. Peripheral penetration depth δ is the reciprocal of the absorption coefficient α of the medium (α = 2k0n'', where k0 is the vacuum wave number and n'' is the imaginary part of the medium refractive index n =ε).

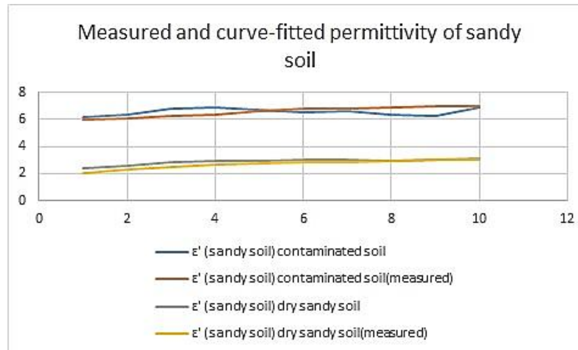

Figure 3: The permittivity of sandy soil versus its frequency before and after contamination

Using equation (1), δ can be calculated and plotted over L-band frequencies, as shown in Fig.4. Due to increased dielectric loss in soil samples that are contaminated, penetration depth will significantly decrease when compared to soil samples that are clean.

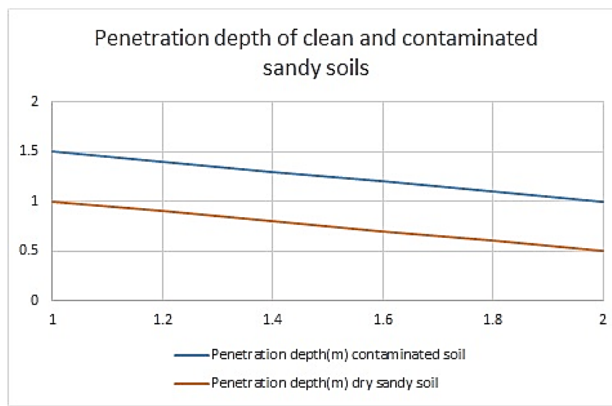

Figure 4: A comparison of the penetration depth of clean and contaminated sandy soils

III. GPR HORN ANTENNA DESIGN

An antenna is the most important component of any GPR system. GPR antennas should have high directivity and efficiency, a wide bandwidth, and proper impedance matching in order to achieve deep penetration and fine resolution [16]. Due to their advantages, horn antennas are the most useful antennas for microwave applications. It is very easy to interface horn antennas with waveguides because they are simple, inexpensive, and easy to manufacture. In addition to their excellent gain and directivity, they are also the best choice for many GPR applications. Due to their high gain, low side and back lobes, simplicity of feeding, and high power handling capabilities, horn antennas are used in the proposed GPR model due to their directivity, gain, and low side and back lobes. In most cases, rectangular waveguide feeders are suitable for rectangular horns. As the electromagnetic wave transitions from the waveguide to free space, the horn facilitates the transition.

GPR antennas cannot penetrate mediums at high frequencies, so the higher the frequency, the less penetration. The resolution of an image will be better with a higher frequency, however. A trade-off must always be made when selecting the optimum GPR frequency. The proposed model is best suited for L-band frequencies to obtain optimal results. Pyramidal horn antennas for soil contamination detection are designed using Ansys HFSS (High-Frequency Structure Simulator) software. A perfect electric conductor (PEC) of 2 mm thickness is assumed to be the material used for designing the pyramidal horn and the waveguide. The waveguide then ensures that microwaves transmitted inside it are reflected appropriately and that surface current does not cause a great deal of Ohmic loss on the surface of the waveguide.

The pyramidal horn antenna structure is shown in Fig.5. In order to connect the antenna to the vector network analyzer (VNA), the antenna is associated with a coaxial adapter, which matches the waveguide to a 50-ohm coaxial cable. The overall optimized dimensions of the designed antenna, obtained utilizing pyramidal horn antenna dimensions' mathematical relationships in [17], are organized in Table.3.

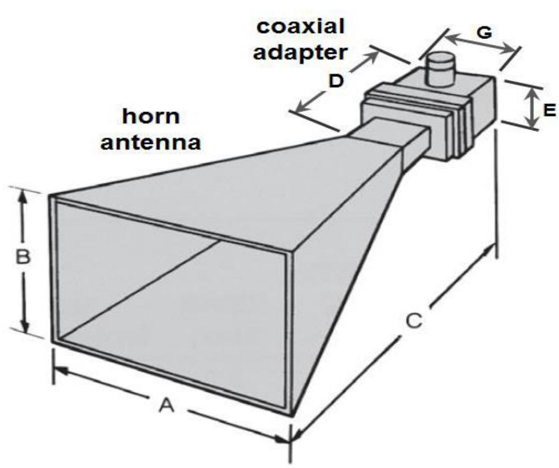

Figure 5: Geometry of the proposed GPR horn antenna

Table 3: Optimized Dimensions of Horn Antenna

Antenna dimensions	**value (cm)**
Aperture width, A	41
Aperture height, B	30
Antenna length, C	80
Waveguide length, D	20
Waveguide height, E	12
Waveguide width, G	24

This is a simulated return loss for the designed GPR horn antenna, S11. At L-band frequencies, the designed horn antenna has a return loss below -12 dB, as shown in Fig.6. The results obtained confirm that most of the power will radiate into space. The designed antenna's polar farfield radiation pattern is shown in Fig.7 at 1, 1.5, and 2 GHz. The waveguide simulations indicate a TE mode with a 415.84 ohm wave impedance. 0.635 GHz is the cutoff frequency, and 28.48 [1/m] is the beta. Based on L-band frequencies, Table.4 shows the gain, beam width, and side lobe level.

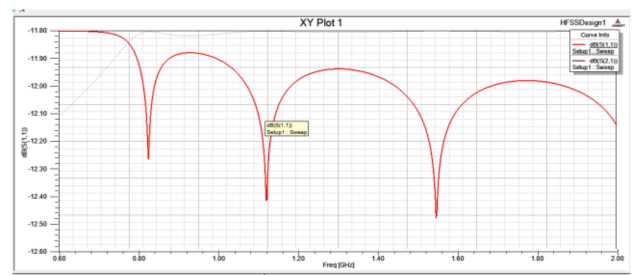

Figure 6: Return loss of designed antenna at L-Band

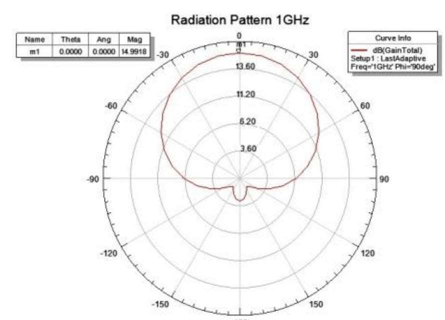

Figure 7a: Gain plot of pyramidal horn antenna obtained at 1GHz

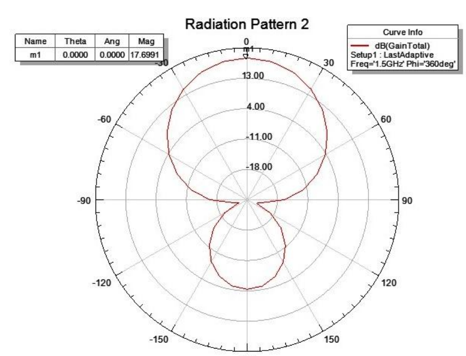

Figure 7b: Gain plot of pyramidal horn antenna obtained at 1.5 GHz

Peer Reviewed & Refereed Journal
Volume-13, Issue-6 (December 2023)
https://doi.org/10.31033/ijemr.13.6.16

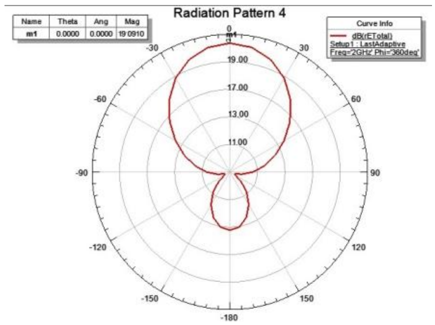

Figure 7c: Gain plot of pyramidal horn antenna obtained at 2GHz

Table 4: Farfield Radiation Parameters over L-Band

Frequency (GHz)	Main lobe Gain (dB)	3-dB Beamwidth (degrees)	Side lobes Level (dB)
1.0	14.9	52.3	-20.0
1.1	12.2	47.4	-22.0
1.2	13.1	42.9	-19.5
1.3	13.8	36.4	-13.3
1.4	14.4	37.4	-17.9
1.5	17.7	32.4	-13.3
1.6	15.4	33.1	-17.3
1.7	15.9	29.1	-12.8
1.8	16.4	29.2	-15.5
1.9	16.7	26.9	-12.8
2.0	19.1	25.9	-13.9

The horn antenna provides a very interesting radiation pattern with a gain of 14.9918 dB, 17.69 dB, and 19.09 dB at 1 GHz, 1.5 GHz, and 2 GHz, respectively; This high gain allows the microwave signals to penetrate deeper into the soil. A low side lobe level and narrow beam width further reduce coupling between transmitting and receiving antennas. Consequently, soil contamination is more easily detected.

IV. RESULTS AND DISCUSSIONS

In GPR, microwave signals are used to detect reflected signals emitted from subsurface structures in order to collect subsurface information. When radiated waves strike buried objects of different dielectric constants, receiver antennas detect variations in their returned signal. Fig.8 illustrates the experimental setup for return loss measurement without obstacles. Fig.9 Illustrates the experimental setup for return loss measurement with obstacles. Mesh-cell structures with a grid resolution of 40 steps per wavelength are used to model antenna structures. In order to provide very precise simulation results, the simulation is performed with 40 dB accuracy.

Figure 8: Experimental setup for return loss measurement without obstacle

Figure9: Experimental setup for return loss measurement with obstacle

A GPR radar can have a monostatic architecture, a bistatic architecture, or a multistatic architecture. Mono-static architectures use a single antenna for transmitting and receiving microwave signals. A bi-static architecture requires two separate antennas for transmission and reception. Multistate radar systems use a single antenna to transmit signals, and multiple antennas to receive them. This study introduces the concept of biostatic radar systems. Direct coupling between transmitting and receiving antennas is an important feature of bi-static radar architecture. It is essential to minimise direct coupling in order to maximise the ability of GPR to discriminate between buried object signals. In order to control the direct coupling, the antennas would need to be spaced (S) and tilted (orientation). An increase in antenna spacing results in a decrease in direct coupling.

As a result, the received reflected signal of the buried object also becomes weaker, and vice versa. There is a significant difference between the reflected signals received from the buried object and the direct coupling at 50 cm of antenna spacing. The direct coupling at this distance is minimised, while the reflected signals are greatly enhanced. A direct coupling is shown in Fig.8 between a transmitting antenna and a receiving antenna over the L-band.

By measuring the change in the electromagnetic coupling between the transmitting and receiving antennas when soil contamination is present, the GPR system can detect soil contamination. An L-band simulation is performed to determine the coupling coefficient, $|S_{21}|$. A realistic simulation setup is implemented in CST Microwave Studio. The first model illustrates oil inside the pipe surrounded by dry sand and dry soil, while the second model shows contaminated sand under the pipe due to oil leaks.

In Fig.9, the coupling coefficient [S_{21}] for the two models is compared with the dimensions introduced in Table.1. Two resonance dips are lower than 12 dB over the entire frequency range, which suggests that antenna impedance matching bandwidth occurs only at these dips. Comparing the results of the contaminated soil model with those of the uncontaminated soil model, a significant increase is seen in the coupling coefficient. The coupling coefficient for both models decreases with increasing frequency as soil attenuation increases with frequency increase. In addition, three different cases are examined: the increase of soil moisture content, the depth at which the pipe is buried, and the change in the spacing between the transmitter and receiver antennas.

4.1 Effect of Soil Moisture

Depending on the operating frequency band as well as the soil conductivity, GPR systems penetrate soil medium. A lower frequency is required for applications that require deep penetration into soil medium. As a result, soils with high electrical conductivity will have a lower penetration depth. Higher conductive soil absorbs energy faster than lower conductive soil. Due to the high concentration of water in moist soil, penetration is much deeper than in dry sand soils. Dry sandy soils are therefore better suited for low-frequency GPR antennas than moist soils. As demonstrated in the previous sub-section, both contaminated and uncontaminated sandy soil have significant contrasts in their reflected signals. According to Fig.10 , it is noticed that the contrast between dry sandy soil and moist sandy soil is no longer significant when the dielectric constant of the soil is 13 and the dielectric loss tangent is 0.29 [18].

Figure 10: S_{21} parameter measurements using VNA

Table 5: Comparison of simulation and real time measurements

Parameter	Simulation Measurement	Real Time Measurement
Wide bandwidth frequency(GHz)	1.6 to 2.7 GHz	1.6 and 2.7 GHz
Return loss(dB)	-12	-14.32 and 18

The high electric conductivity of moist soil makes it likely that |S21| is lower than that of dry soil. According to the results, oil contaminants can be detected effectively in sandy soils, whereas in wet soils detection becomes impossible [19, 20].

4.2 Effect of Pipe Burial Depth

In Fig.10, the coupling coefficient, $|S_{21}|$, is shown as a function of increasing the depth (D) at which the pipe is buried from 40cm to 50cm, while keeping all other dimensions constant. Regardless of soil contamination, the coupling coefficient $|S_{21}|$ decreases as pipe burial depth increases. The antenna radiation pattern reduces the received signal from the contaminated soil layer as the antenna-to-ground spacing increases. Accordingly, contaminated areas near the surface of the ground are easier to detect. In contaminated areas, attenuation increases significantly, thus decreasing the backscattered power. Therefore, deeper soil contamination is more difficult to detect.

4.3 Effect of Antenna Spacing

In order to achieve the best soil contamination detection, it is critical to determine the spacing between the transmitting and receiving antennas (S) and the tilt (orientation) of the antennas. This direct coupling ought to be minimised for the best soil contamination detection. A decrease in direct coupling is observed as the spacing between the two antennas increases. As a result, the reflected signal from the contaminated soil also becomes weaker. It is recommended to place the transmitter and receiver antennas 50cm apart to minimise direct coupling and to amplify reflected signals received from contaminated underground soil. The direct coupling between the transmitting and receiving antennas is increased by lowering the antenna spacing (S) from 50 cm to 40 cm while maintaining all other dimensions as in Table.1. For the clean and contaminated soils, the comparison is presented over their entire frequency range, displayed in Table.1. Due to the decrease in direct coupling between the two antennas, as the antenna spacing increases, considerable increases in $|S_{21}|$ occur at the resonance dips of soil models.

V. CONCLUSION AND FUTURE WORK

GPR can be used to detect soil contamination caused by oil leaks from underground pipelines, and this study examines its validity and effectiveness. Based on full-wave electromagnetic simulations, we analyzed the analytical aspects and design considerations of a prototype pipe filled with lubricant oil and buried in sandy soil. Using the model, electromagnetic measurements taken in contaminated soil are evaluated. For bi-static GPR systems, two identical horn antennas operating at L-band frequencies have been developed. As a result of this design, it has been determined that there is a noticeable difference between the reflected signal in the presence and absence of oil leaks. Three parameters are highly dependent on the performance of the GPR system in this study: soil moisture content, pipe burial depth, and antenna configuration. According to the results, soil contamination can be detected using the GPR system. There is enormous potential for further research in the work described in this paper.

As a result of the current research, the following possibilities may arise:

A pyramidal horn antenna was designed, fabricated, and its parameters measured, and compared with simulated values.

1) *Performing the real-world laboratory experiments of the soil contamination detection model exhibited in the current study and comparing the laboratory measurements with the simulated results presented in this work.*

2) *Investigation of this study utilizing a multi-static radar architecture where multiple receiving antennas in an array configuration are used for the receiving of signals and comparison of the results with the current study*

3) *Investigation of this study utilising multi-static radar architecture where multiple receiving antennas in an array configuration are used for the receiving of signals and comparison of the results with the current study*

Acknowledgment
None.

Conflicts of Interest
The authors have no conflicts of interest to declare.

REFERENCS

[1] Yi Tan, Arwa Abdulkreem Al-Huqail, Qiusong Chen, Hasan Sh. Majdi, Jari S. Algethami, & Haitham Elhosiny Ali. (2022). Analysis of groundwater pollution in a petroleum refinery energy contributed in rock mechanics through ANFIS-AHP. *International Journal of Energy Research*. https://doi.org/10.1002/er.8663.

[2] Christian Riboldi, Danilo A. Carnevale Castillo,Daniele M. Crafa & Marco Carminati. (2023). *Contactless sensing of water properties for smart monitoring of pipelines in sensors*.

[3] Pringle, J.K, Stimpson, I.G, Wisniewski, K.D, Heaton, V, Davenward, B, Mirosch, N, Spencer, F & Jervis, J.R. (2020). *Geophysical monitoring of simulated homicide burials for forensic investigations in Scientific reports, 2020*. https://link.springer.com/content/pdf/10.1038/s41598-020-64262-3.pdf.

[4] Jesús García Sánchez,José Manuel Costa-García,João Fonte & David González-Álvarez. (2022). *Exploring ephemeral features with ground-penetrating radar: An approach to Roman military camps in remote sensing*. https://doi.org/10.3390/rs14194884.

[5] Rosmadi Ghazali, Abdul Rauf & Abdul Rasam. (2019). Estimation of different subsurface materials depth using Ground Penetrating Radar. *International Journal of Advanced Trends in Computer Science and Engineering*. DOI: 10.30534/ijatcse/2019/6581.32019.

[6] Ahmad H. Abdelgwad, Tarek M. Said & Amr M. Gody. (2015). Developing of a ground penetrating radar antenna for detecting water pollution in underground pipelines. *International Journal of Microwaves Applications*. http://warse.org/pdfs/2015/ijma01412015.pdf.

[7] Saeed Parnow, Hamid Bizhani & Mahdy Zarei. (2020). Application of ground penetrating radar (GPR) to discover water table. In: *19th Iranian Geophysical Conference*.

[8] Galih Prasetya Dinanta, Noviarso Wicaksono, Wahyu Hidayat, Rachmat Ramadhan, Muhammad Rifat Noor, Daniel Cassidy, Yanto Sudiyanto, Eddy Heraldy, Afifuddin & Muhammad Razzaaq Al Ghiffary. (2023). Case study of ground penetration radar (GPR) to assess lead migration. *Results in Geophysical Sciences*.

[9] A Ball & L O'Connor. (2021). *Geologist in the loop: a hybrid intelligence model for identifying geological boundaries from augmented ground penetrating radar in Geosciences*.

[10] GPH Ching, RKW Chang, TXH Luo & WWL Lai. (2021). *GPR virtual guidance system for subsurface 3D imaging in Remote Sensing*.

[11] Teerapon Yodrot,Samran Santalunai,Chanchai Thongsopa,Thanaset Thosdeekoraphat & Nuchanart Santalunai. (2023). *Measurement of dielectric properties in soil contaminated by biodiesel-diesel blends based on radio frequency heating", in applied sciences*.

[12] Ivo Petrov, Oksana Kalinkevich, Maksym Pogorielov, Aleksei Kalinkevich, Aleksandr Stanislavov, Anatoly Sklyar, Sergei Danilchenko & Temenuzhka Yovcheva. (2016). *Dielectric and electric properties of new chitosan-hydroxyapatite*

materials for biomedical application: Dielectric spectroscopy and corona treatment. https://doi.org/10.1016/j.carbpol.2016.05.110.

[13] Xinran Wang, Hongfu Guo, Chen Zhou & Junkai Bai. (2021). High-resolution probe design for measuring the dielectric properties of human tissues. *BioMedical Engineering*. https://doi.org/10.1186/s12938-021-00924-1r.

[14] Xingqian Xu, Haijun Wang, Xin Qu & Cheng Li. (2022). Study on the dielectric properties and dielectric constant model of laterite. *Frontiers in Earth Science*. https://doi.org/10.3389/feart.2022.1035692.

[15] Priyanka Shaw, Naresh Kumar, Sohail Mumtaz, Jun Sup Lim, Jung Hyun Jang, Doyoung Kim, Bidya Dhar Sahu, Annemie Bogaerts & Eun Ha Choi. (2021). Evaluation of non-thermal effect of microwave radiation and its mode of action in bacterial cell inactivation. *Nature Scientific Reports*. https://doi.org/10.1038/s41598-021-93274-w.

[16] Jawad Ali, Noorsaliza Abdullah, Muhammad Yusof Ismail & Ezri Mohd, S.M. Shah. (2017). Ultra-wideband antenna design for gpr applications: A review. *International Journal of Advanced Computer Science and Applications*. DOI: 10.14569/IJACSA.2017.080753.

[17] Constantine A. Balanis. (2016). *Antenna theory: Analysis and design*. (4th ed.).

[18] Mohammad Riahi & Amirhossein Tavangar. (2008). Prognosis of the Effects of soil characteristics on the performance of landmine detection in ground-penetrating radar system - a case study. *The 2nd International Conference on Technical Inspection and NDT*. https://www.ndt.net/search/docs.php3?id=7605.

[19] I.Frau,S. R. Wylie,P. Byrne, J. D. Cullen, O. Korostynska & A. Mason. (2020). Functionalised microwave sensors for real-time monitoring of copper and zinc concentration in mining-impacted water. *International Journal of Environmental Science and Technology*. https://doi.org/10.1007/s13762-019-02588-w.

[20] Yajian Wang, Pengpeng Li & Jianfeng Li. (2022). The monitoring approaches and non-destructive testing technologies for sewer pipelines. *Water Science & Technology*. https://doi.org/10.2166/wst.2022.120.